

Control of shape memory alloy actuator using pulse width modulation

N Ma and G Song

Smart Materials and Structures Laboratory, Department of Mechanical Engineering,
University of Houston, Houston, TX 77204, USA

Received 25 February 2002

Published 25 September 2003

Online at stacks.iop.org/SMS/12/712

Abstract

Shape memory alloys (SMA), in particular nickel–titanium alloy (or nitinol), have been used as actuators in some astronautic, aeronautic and industrial applications. The future will see more SMA application if less energy is required for actuation. This paper presents the design and experimental results of control of an SMA actuator using pulse width modulation (PWM) to reduce the energy consumption by the SMA actuator. A SMA wire test stand is used in this research. Open-loop testing of the SMA wire actuator is conducted to study the effect of the PWM parameters. Based on test results and parameter analysis of the pulse width (PW) modulator, a PW modulator is designed to modulate a proportional plus derivative (PD) controller. Experiments demonstrate that control of the SMA actuator using PWM effectively saves actuation energy while maintaining the same control accuracy as compared to continuous PD control. PWM also demonstrates robustness to external disturbances. A comparison with a pulse width pulse frequency modulator is also presented.

(Some figures in this article are in colour only in the electronic version)

1. Introduction

Shape memory alloy (SMA), in particular nickel–titanium alloy (or nitinol), is a smart material that has the ability to return to its predetermined shape when heated above a certain temperature. The ‘memory’ of the predetermined shape is resulted from the crystal structure transformation from martensite to austenite. This transformation can be caused by thermal heating or electrical resistance heating. An SMA actuator can yield an extremely large force if it encounters any external resistance during this phase transformation. For instance, a nitinol wire 0.02 inches in diameter can generate 16 pounds of force. During its free movement, an SMA actuator can generate 8% of strain for a single use or 5% strain for repeated operations. Furthermore, SMAs can be fabricated into different shapes. These properties make SMA actuators suitable for a variety of applications.

However, the low energy efficiency in electrical resistance actuation of SMAs obstructs the wider application of SMA. It is of great interest to improve the energy efficiency of electrical resistance actuation of SMA actuators. Though modulation techniques are commonly used to reduce energy consumption in electric drive systems, control of SMA actuators using modulation techniques are not well addressed in the literature.

There are several modulation techniques, such as pseudo-rate modulation (Millar and Vigneron 1976), integral-pulse frequency modulation (Clark and Franklin 1969, Hablani 1994), pulse width modulation (PWM) (Kempski *et al* 2001) and pulse width pulse frequency (PWPF) modulation (Bittner *et al* 1982, Wie and Plescia 1984, Anthony *et al* 1990, Song *et al* 1999, Song and Ma 2001). Among these modulators, PWM has the advantages of being robust to disturbances, effective in saving energy and easily implemented using microprocessors. Therefore, PWM has found many applications, such as motor controls, spacecraft controls (Anthony *et al* 1990), air jet control (Zhao and Jones 1997) and pneumatic systems (Shih and Ma 1998, Noritsugu *et al* 1986). PWM has been applied to micro-robots actuated by SMA materials (Honma *et al* 1984, Kato *et al* 1999). These are the only few articles discussing PWM for SMA actuator in the literature. This motivates the authors to conduct research in designing PWM modulated controller for position control of SMA actuators.

This paper presents a detailed pulse width (PW) modulator design for SMA actuators based on experimental results. A comparative study of PWM, PWPF, and continuous controls is also conducted. SMA wire actuators are used in this research and a SMA wire testing platform is fabricated. To assist the

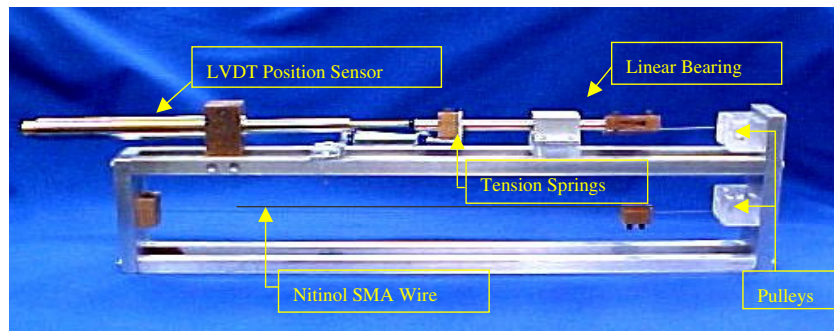


Figure 1. The experimental set-up.

design of the PW modulator, open-loop tests of the SMA wire are first conducted. Then tests of the SMA wire under PWM with different modulator parameters are performed to reveal the effect of each parameter on the actuator's performance. Based on these tests, a PW modulator is designed to modulate a proportional plus derivative (PD) controller for position control of the SMA wire actuator. In order to compare the effect of PWM in energy saving, experiments on position control of the SMA wire actuator using a regular PD controller, a PWPF-modulated PD controller and a PW-modulated PD controller are conducted. Experimental results show that with the PW-modulated PD controller the SMA wire actuator consumes 30% less energy than in the case with the continuous PD controller, while maintaining the same positioning accuracy.

2. The experimental set-up

The experimental set-up was designed to allow the position control of a single SMA wire. This set-up (see figure 1) consists of four major components: a SMA wire actuator, a spring–slider device, a sensor and a stand frame. The actuator is a single SMA wire (22.86 cm in length and 0.381 mm in diameter), with one end connected to a nonconductive cable and the other to a nonconductive support. The support is fixed to the frame of the stand. The cable is linked to a spring–slider device via two pulleys. The slider moves in a horizontal direction supported by a linear bearing. When the wire is heated and then contracts, the slider will be pulled forward, and the bias spring will pull it back after the wire has cooled. The spring also applies pretension to the SMA wire. The linear variable differential transformer (LVDT) whose tip is forced against the slider detects the displacement of the slider.

To control the position of the wire, control systems are designed and implemented by using a Matlab/Simulink and dSPACE data acquisition system. The output voltage, which is 10 times the original value of modulator output being amplified by the dSPACE D/A converter, is sent to the power supply. The power supply amplifies the voltage by a factor of four and applies this voltage to the SMA wire. The current through the wire results in the heating process of the wire and leads to phase transformation when the temperature of the wire is above the transformation temperature. The wire contracts, resulting in movement of the slider and additional tension on the spring via the cable. The displacement of the slider is measured by the LVDT and fed back to the control system. Once the voltage is

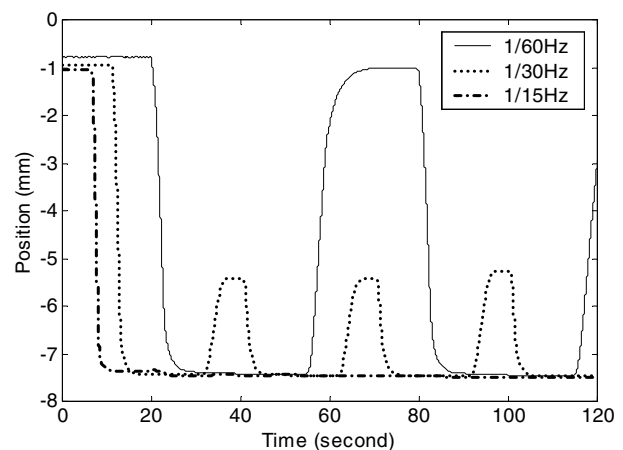


Figure 2. Position responses with different sinusoidal inputs.

shut off and the wire has cooled, the bias spring pulls back the slider to its original position.

3. Open-loop testing of the SMA wire actuator

It is necessary to investigate some of the SMA wire actuator's basic properties, like the response time and the maximum displacement, since these data will provide useful information in the design of the PW modulator and the PD controller.

First, the SMA wire actuator was tested with sinusoidal inputs of different frequencies at 1/60, 1/30 and 1/15 Hz, respectively. The position response of the SMA wire is shown in figure 2. In this plot, it is obvious that the SMA wire actuator moves from its original position (in martensite) at around -1 mm to its peak position (in austenite) at -7.4 mm, and that the 1/15 Hz commanding signal is too fast for SMA actuator to cool and 1/60 Hz is the upper limit frequency for actuator to response properly.

Second, three square wave signals at 1/60, 1/30 and 1/15 Hz are used to test SMA for responses to step input and response time. The square wave signals have the same range of amplitude as in the previous case. Figure 3 shows the position responses of the wire. It is noticed that it takes 8 s for the SMA wire to reach the final value during heating and about 13 s for it to retract 62% to its original position. Therefore, it is reasonable to estimate the time constant for the heating process is 2 and 13 s for cooling if simply modeling the SMA by two first-order dynamic processes separately.

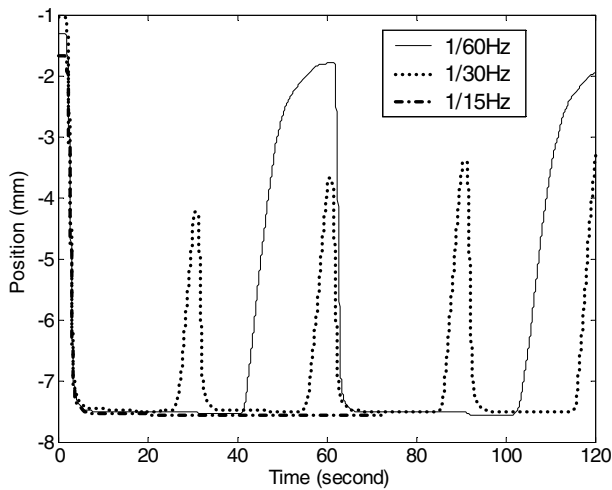


Figure 3. Position responses with different square wave inputs.

4. Design of PWM modulator

4.1. Introduction to PWM

When a PW modulator is integrated into a feedback control system, it is able to bring robustness to the system and to reduce the energy needed in driving actuators due to its approximation of an average behavior of a continuous command by using a discontinuous pulse signal.

There is a variety of mechanisms to realize PWM. The PW modulator adopted here is illustrated in figure 4. It is comprised of a carrier wave generator, a bang–bang trigger, a gain block and a saturation block. The carrier wave generator produces a triangular carrier wave with a constant frequency and amplitude greater than the maximum values of those of the command signal. At the sum block, the command signal is subtracted by the carrier wave and then the difference is input into the bang–bang trigger. If this difference is positive and larger than the threshold of the bang–bang trigger, the bang–bang trigger outputs a constant value d (indicated in figure 4) corresponding to the on-state; otherwise, its output is at the off-state and outputs a corresponding constant value $d - h$ (indicated in figure 4). The bang–bang trigger switches twice in each period of the triangular carrier wave, and the pulse width (PW) is equal to the time interval during which the difference is larger than the threshold. Therefore, a pulse sequence is generated. This pulse sequence has the same frequency as the carrier wave and constant amplitude. This amplitude is equal to the amplified on-state output of the bang–bang trigger. The gain block is used to amplify the output of the bang–bang trigger, and the saturation block limits the maximum output for safety reasons.

To illustrate the operation of the PW modulator, let us consider an example of a sine wave modulator. In this modulator, the threshold of the bang–bang trigger is set to zero. The outputs of the trigger at on- and off-state are set to be one and zero, respectively. Moreover, the carrier wave is a triangular wave with a frequency of 6.7 Hz and amplitude of two. The sine wave signal (0.5 Hz frequency and 1 magnitude) is modulated to a pulse signal, which has magnitude of one at on-time and zero at off-time (gain is equal to one). The sine

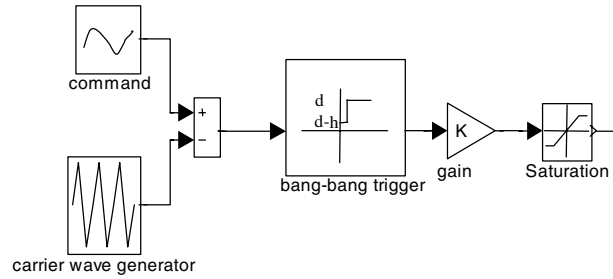


Figure 4. The implementation of PWM.

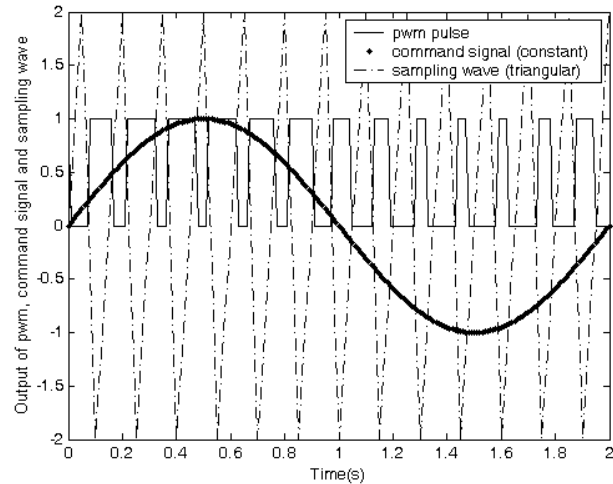


Figure 5. Sinusoid signal and modulated pulse.

wave signal and the modulated signal are shown in figure 5. Using different values of the threshold and outputs at on- and off-state of bang–bang trigger leads to different types of pulse signals.

4.2. Static analysis of PWM

To explore the relationship of the PW and amplitude of the command signal, the static characteristics of the PW modulator is investigated first.

Figure 6 illustrates how a PW modulator works to transform a constant command signal $W(t)$ into a pulse signal $Z(t)$. The amplitude of the carrier wave is supposed to be greater than that of the signal $W(t)$. The average output of the PW modulator is given by Zhao and Jones (1997):

$$\overline{z(t)} = \frac{A_{\text{PWM}}}{A_{\text{carrier}}} \overline{W(t)} \tag{1}$$

where A_{PWM} is the amplitude of the output of the PWM modulator and A_{carrier} is the amplitude of the carrier wave. The $\overline{z(t)}$ is the average output of the PWM, while $\overline{W(t)}$ is the average of the command signal. Here the average of output of PWM and the command signal are time averages in one period of the carrier wave.

Since the ratio of the amplitudes of the PW modulator output and carrier wave does not depend on the time, the average output of the PW modulator is proportional to the average of the command signal. Furthermore, the time average of the square pulse is only determined by the PW. Therefore,

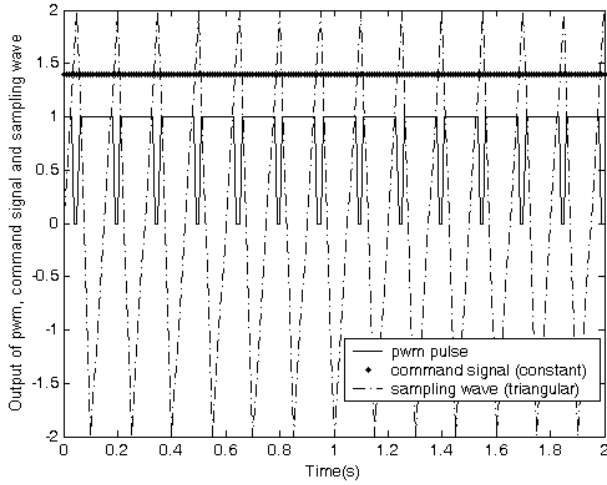


Figure 6. A constant signal and its modulated pulse.

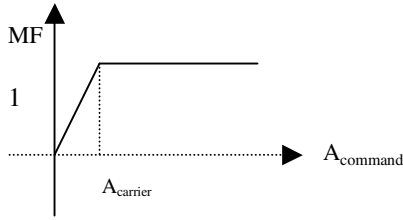


Figure 7. Relationship of MF and the amplitude of the command signal and the carrier wave.

it is concluded that the PW is proportional to the amplitude of the constant command.

The time taken by the output of the bang–bang trigger to move from d to $d - h$ is defined as the on-time or PW, denoted by T_{on} ; the off-time is defined as the time taken by the output of the bang–bang trigger to move from $d - h$ to d . The on-time and off-time in each period are given by

$$T_{on} = \frac{A_{command}}{A_{carrier}} P_{carrier} = \frac{A_{command}}{A_{carrier}} \frac{1}{f_{carrier}} \quad (2)$$

$$\begin{aligned} T_{off} &= \frac{A_{carrier} - A_{command}}{A_{carrier}} P_{carrier} \\ &= \frac{A_{carrier} - A_{command}}{A_{carrier}} \frac{1}{f_{carrier}} \end{aligned} \quad (3)$$

where $A_{command}$ is the magnitude of the command signal, $P_{carrier}$ and $f_{carrier}$ are the period and the frequency of the carrier wave respectively.

The modulation factor (MF) of the PW modulator is defined as the ratio of the on-time to the period and is described by

$$MF = \frac{T_{on}}{T_{on} + T_{off}} = \frac{A_{command}}{A_{carrier}}. \quad (4)$$

Another commonly used parameter of the PW modulator, the duty cycle, is expressed in the percentage format of the MF.

If the frequency of the carrier wave is much higher than that of the time-varying command signal, the command signal can be considered piecewise constant in each period and the PW is approximately proportional to the varying magnitude of the command signal. For the time-varying command signal, the relationship of MF and the command amplitude is shown in figure 7.

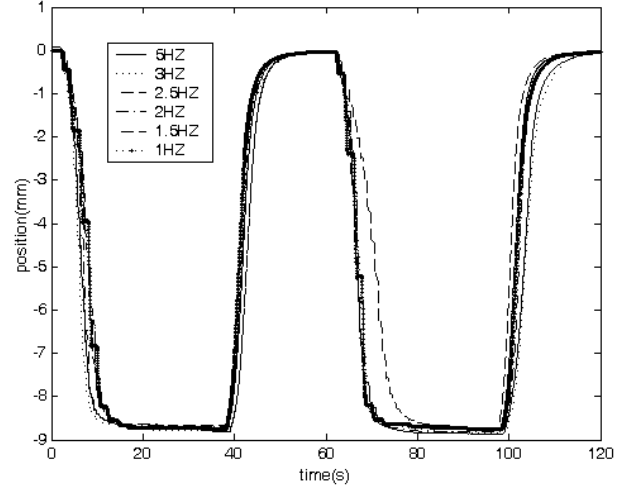


Figure 8. Position responses by one-way PWM of different frequencies.

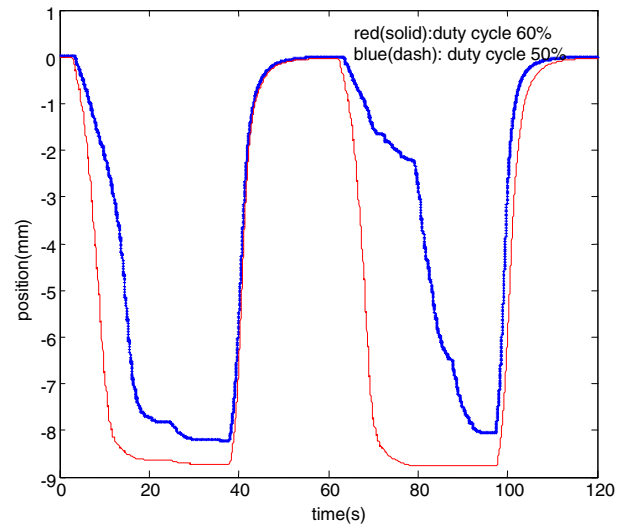


Figure 9. Position responses in open-loop tests using one-way PWM.

4.3. Design of PW modulator

The design of a PW modulator involves determination of the threshold of the bang–bang trigger, the output of the bang–bang trigger, the amplitude and the frequency of the carrier wave.

A type of PW modulator called a one-way PW modulator is used in this paper to achieve the greatest saving energy. The one-way PW modulator applies a pulse sequence of voltage to the SMA actuator only when there is a positive control signal. Otherwise, the output of the PWM is zero to cut off the power to the SMA actuator. Therefore, since the command signal to the bang–bang trigger of the one-way PWM is the output of a PD controller, the threshold of the one-way PWM is zero and output of the bang–bang trigger in the off-state is zero. In addition, the carrier wave has non-negative magnitude and amplitude of output of the PWM modulator is 0.075, which corresponds to the 3.0 V voltage required to actuate the SMA wire actuator, according to the experimental results.

Since the output of the PD controller is a time-varying signal, as discussed in the previous section, the frequency of

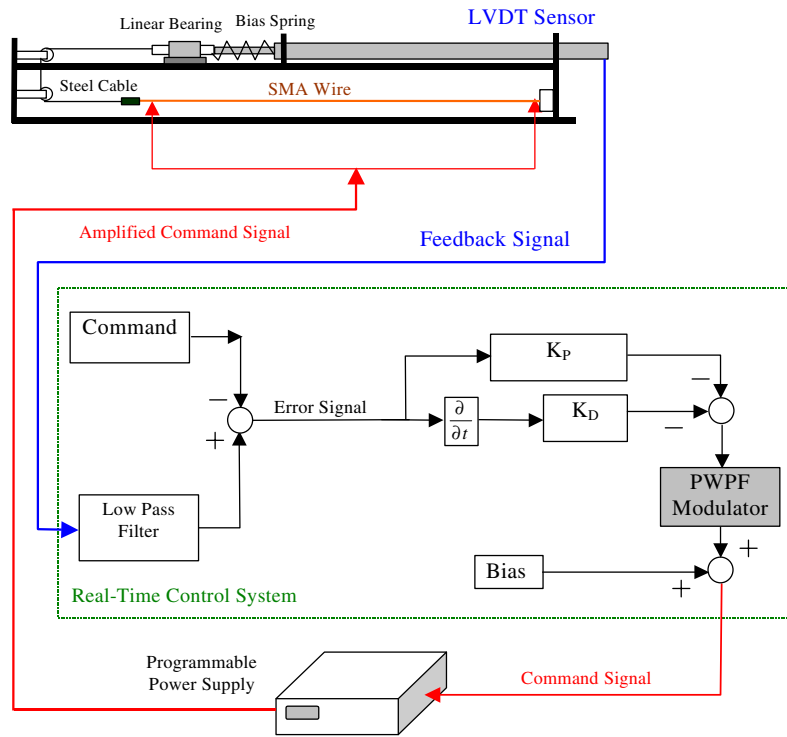


Figure 10. Block diagram of the feedback control system.

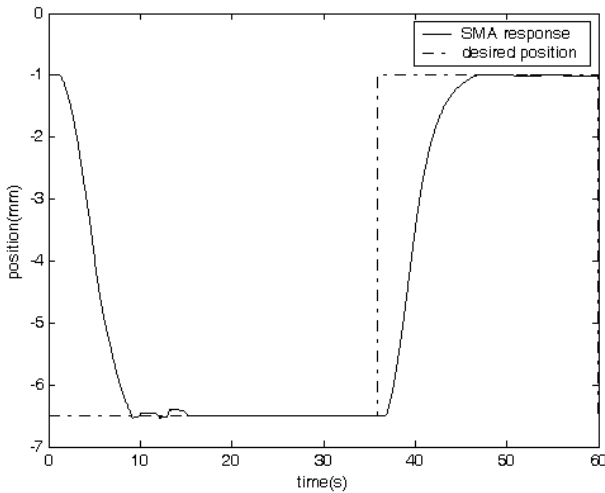


Figure 11. Position response with the PW-modulated PD control.

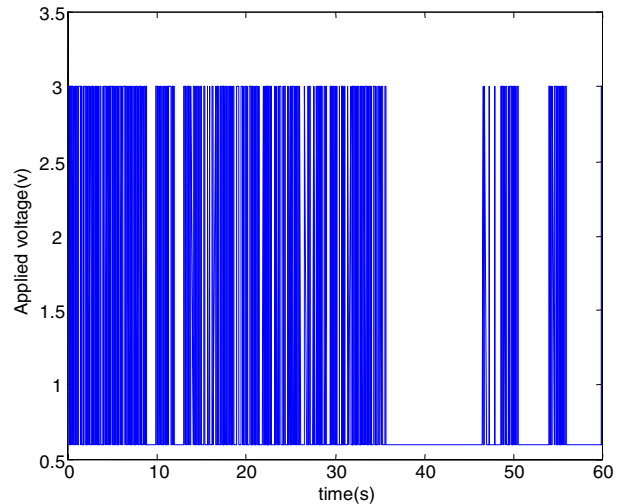


Figure 12. Applied voltages with the PW-modulated PD control.

the carrier wave must be much higher than that of the output of the PD controller. On the other hand, a higher frequency of the PW modulator pulse will result in more energy consumption. Therefore, to obtain the appropriate frequency of the PW modulator pulse, several open-loop tests on the SMA actuator using one-way PWM were conducted.

The experimental results are shown in figure 8. The pulse signals used in tests have frequencies of 5, 3, 2.5, 2, 1.5 and 1 Hz. From the plot, it can be seen that the position responses of the SMA actuator are similar. Therefore, in this application of the PW modulator, a PW modulator with a low frequency has the same ability to drive the SMA actuator as a PW modulator with a high frequency.

According to the open-loop testing on the SMA actuator, the SMA actuator can only respond to an input with frequency greater than 1/15 Hz in air. Therefore, the frequency of the PW modulator pulse is set to be 10 Hz, which is significantly larger than that of the possible command signal and has a satisfactory energy-saving efficiency.

Finally, the range of duty cycle is carefully chosen to achieve the goals of high energy efficiency and a quick response simultaneously. The figure 9 shows that the position responses of the SMA actuator when the one-way PWM is employed in open-loop tests. The experimental results show that when the width of the pulse is smaller than 50%, the time for heating the SMA wire is too little to actuate the SMA actuator. Therefore,

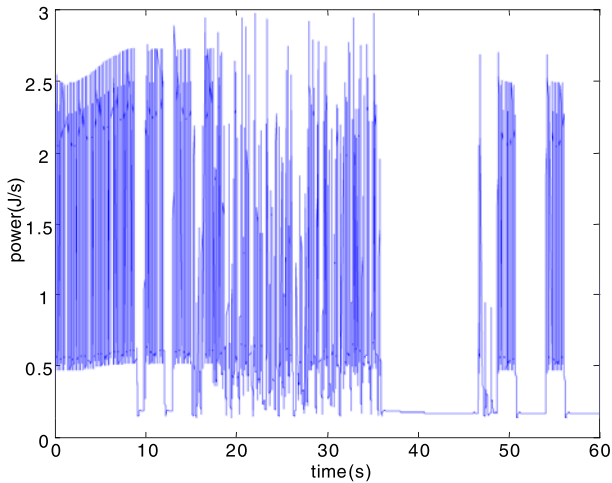


Figure 13. Power consumption of the PW-modulated PD control.

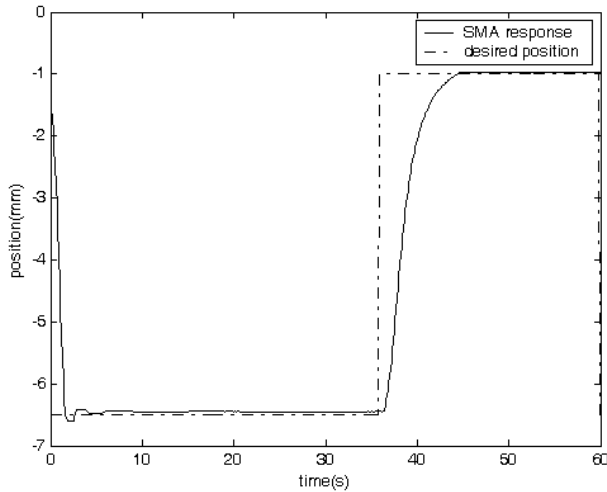


Figure 14. Position response with the PWPF-modulated PD control.

the minimum duty cycle of the pulse is 50%. On the other hand, to make the SMA actuator respond quickly, the maximum duty cycle of the PWM pulse train is set to be 91%.

From equation (4), the amplitude of the carrier wave can be determined as the range of MF goes from 0.5 to 0.91, given the maximum control signal measured in the tests. On the other hand, the desired range of MF can be obtained by adjusting the amplitude of carrier wave.

5. Control of SMA position using PW-modulated PD controller

A PD controller and the PW modulator were designed to implement the position control of the SMA wire actuator (figure 1). The control system is illustrated in figure 10. For the PD controller, the proportional gain is 0.51 and derivative gain is 0.07. The PW modulator transforms the output of the PD controller into a pulse sequence and provides both robustness to external disturbances and energy saving.

The PWM pulse has a magnitude of 3.0 and a frequency of 10 Hz, with the duty cycle being restricted to a range from 50 to 91%.

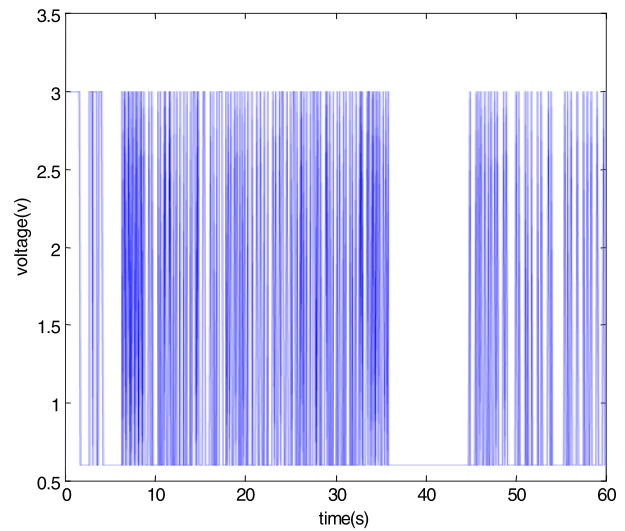


Figure 15. Applied voltages of the PWPF-modulated PD control.

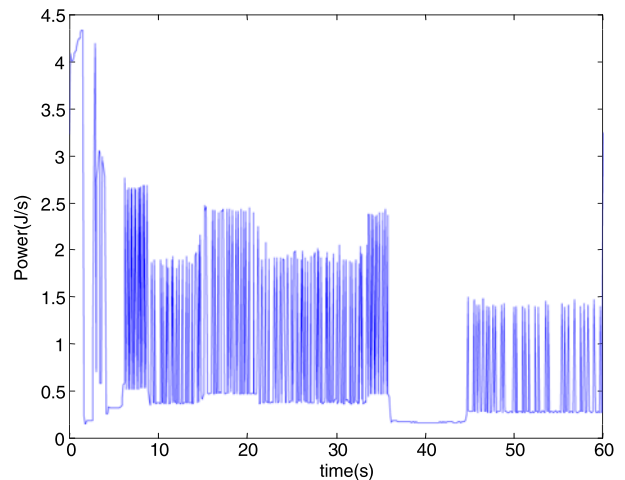


Figure 16. Power consumption of the PWPF-modulated PD control.

6. Experimental results

First, experiments on position control by the PW-modulated PD controller were carried out. The desired position command is a square wave signal (1/60 Hz, 60% duty cycle, from -1 to -6.5 mm). The position response, applied voltage and power consumption of the SMA actuator are shown in figures 11–13. Then, for comparison purposes, experiments using the PWPF-modulated PD control and the continuous PD control were conducted, all under the same conditions (i.e. the proportional gain and derivative gain remained the same). Figures 14–19 show the position response, applied voltage and power consumption of the SMA driven by the PWPF-modulated PD control and the continuous PD control, respectively.

Four criteria were selected to evaluate the performance of these different controllers. These criteria are the energy consumption, the mean value and the standard derivation of the steady-state error and the setting time. If using a first-order system to mimic the heating process of the SMA actuator. The setting time is defined as the time for the SMA actuator to reach and stay within a specified range of the desired

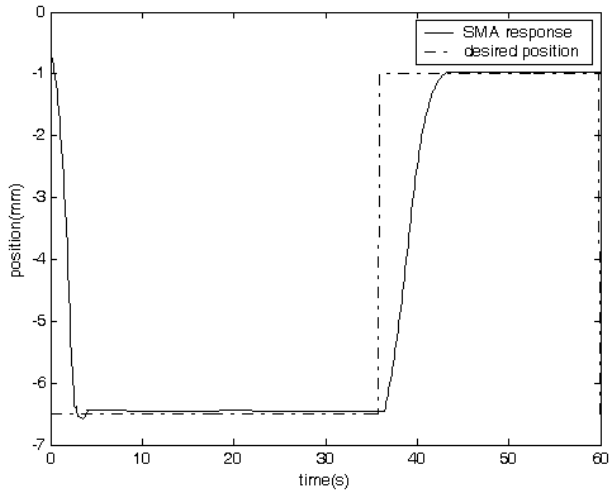


Figure 17. Position response with the continuous PD control.

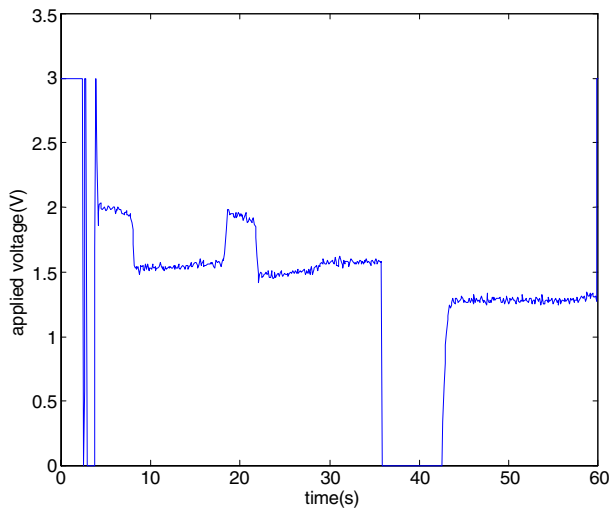


Figure 18. Applied voltages with the continuous PD control.

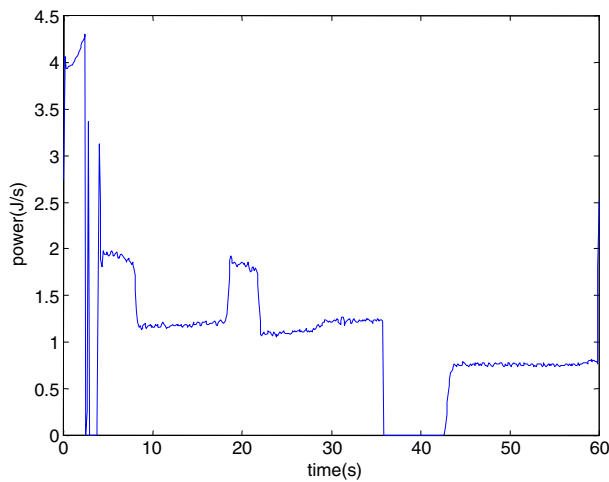


Figure 19. Power consumption of the continuous PD control.

position. Generally, this range has a size of 2% of the desired displacement value. As the desired stroke of the SMA actuator is -5.5 mm, the steady-state range around the desired position

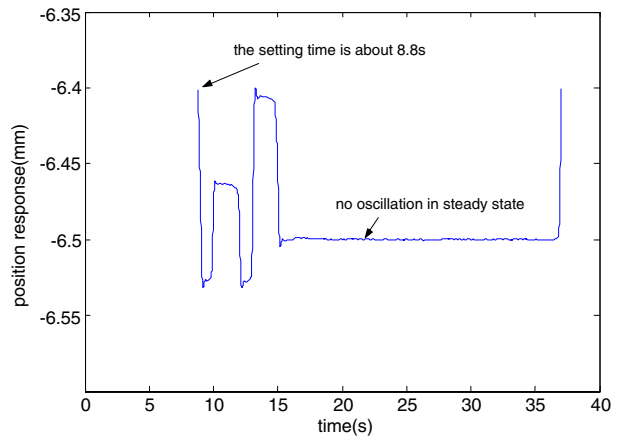


Figure 20. Close-up view—steady state of position response with the PW-modulated PD controller.

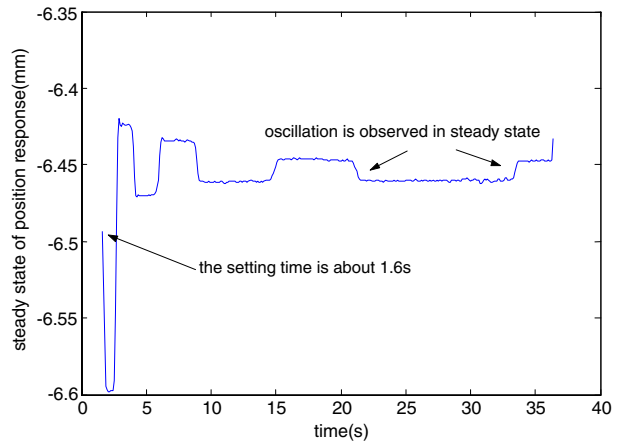


Figure 21. Close-up view—steady state of position response with the PWPF-modulated PD controller.

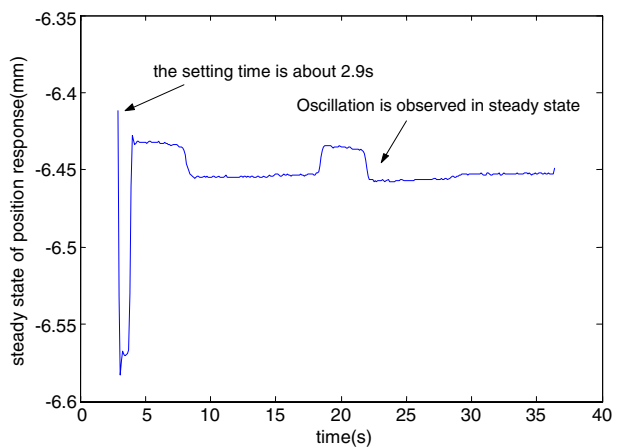


Figure 22. Close-up view—steady state of position response by the regular PD controller.

in heating process is from -6.6 to -6.4 mm. Figures 20–22 respectively show the close-up views of steady states of the SMA actuator controlled by these three controllers. In addition, the results are summarized in table 1. From the data in table 1 and figures 20–22, it is obvious that both the PWPF-modulated PD controller and the continuous PD controller

Table 1. Comparison of performance of the PW-modulated PD controller, the PWPF-modulated PD controller and the continuous PD controller.

	PWM	PWPF	Continuous PD
Energy consumption (J)	47.19	50.76	66.58
Standard of error (mm)	0.0259	0.0233	0.0205
Mean of error (mm)	-0.0078	-0.0233	-0.0475
Setting time (s)	8.8	1.6	2.9

maintain similar position control accuracy, while the PWM-modulated PD controller achieves a more accurate position control. Moreover, the energy consumption by the PWM modulated PD controller is the least among the three controllers and is 30% less than that of the continuous PD controller. On the other hand, the PWPF-modulated PD controller provides the fastest response because its frequency can be adjusted and it behaves like a continuous signal at the beginning of activation. Although it takes about 8.8 s for the SMA actuator driven by the PWM to reach the steady state, the PW-modulated PD controller adds robustness to the system. Since the SMA wire actuator is exposed to an open environment, it is subject to changes in convection conditions. These environmental disturbances often cause the wire actuator to oscillate around its final position. It is impressive to see from figure 20 that there is no oscillation in case of the PW modulator, while figures 21 and 22 clearly show oscillations in the other two cases. Therefore, we can conclude that the PW-modulated PD control has the advantage of being more stable and robust than the PWPF-modulated PD control or the regular PD control, in addition to its advantage in energy saving.

7. Conclusion and discussion

The experiments in this paper demonstrate the position control of an SMA wire actuator using a PW-modulated PD controller. An experimental comparative study of the PW-modulated PD control, PWPF-modulated PD control, and a continuous PD control is conducted. The PW modulator has advantages of saving energy as well as improving the system's robustness to external disturbances. The performance of the PW modulator is comparable to that of a continuous controller in terms of control accuracy, but offers dramatic energy saving. Moreover, the PW modulator is easier to implement than the PWPF modulator. Future work will involve implementation of a PW modulator using a microprocessor to minimize the controller so that it can be integrated into smart structure systems.

Acknowledgments

The authors would like to acknowledge the support provided by NSF via a CAREER grant and NASA via a cooperative grant.

The authors are grateful for the contributions from Mr Todd Barr and Mr Nick Penney in design and fabrication of the experimental set-up. Mr Dale Ertley's effort of machining some key components of the experimental set-up is also greatly appreciated.

References

- Anthony T, Wei B and Carroll S 1990 Pulse-modulated control synthesis for a flexible spacecraft *AIAA J. Guid. Control Dyn.* **13** 1014–22
- Bittner H, Fischer H D and Surauer M 1982 Design of reaction jet attitude control systems for flexible spacecraft *IFAC Automatic Control in Space* (The Netherlands: Noordwijkerhout)
- Clark R N and Franklin G F 1969 Limit cycle oscillations in pulse modulated systems *J. Spacecr. Rockets* **6** 799–804
- Hablani H B 1994 Multiaxis tracking and attitude control of flexible spacecraft with reaction jets *AIAA J. Guid. Control Dyn.* **17** 831–9
- Honma D, Miwa Y and Iguchi N 1984 Micro manipulators applied shape memory effect *J. Japan Soc. Precis. Eng.* **50** 377–82
- Kato T, Tamura K and Yamamoto R 1999 Hexapod walking microrobot with actuator using shape memory alloy *Research Reports* No 86 Kogakuin University pp 5–10
- Kempski A, Strzelcki R, Smolenski R and Fedyczak Z 2001 Bearing current path and pulse rate in PWM-inverter-fed induction *2001 IEEE 32nd Annual Power Electronics Specialists Conf. (Vancouver, Canada)* vol 4 (Piscataway, NJ: IEEE) pp 2025–30
- Millar A and Vigneron F R 1976 Attitude stability of flexible spacecraft which use dual time constant feedback lag network pseudorate control *AIAA/CASI 6th Communications Satellite Systems Conf. (Montreal, Canada, April 1976)*
- Noritsugu T 1986 Development of PWM mode electro-pneumatic servomechanism, part I: speed control of a pneumatic cylinder *J. Fluid Control* **7** 65–80
- Shih M and Ma M 1998 Position control of a pneumatic cylinder using fuzzy PWM control method *Mechatronics* **8** 241–53
- Song G, Buck N and Agrawal B 1999 Spacecraft vibration reduction using pulse-width pulse-frequency modulated input shaper *AIAA J. Guid. Control Dyn.* **22** 433–40
- Song G and Ma N 2001 Control of shape memory alloy actuators using pulse width pulse frequency (PWPF) modulation *Proc. 2001 Int. Mechanical Engineering Congr. and Exposition (Nov. 2001)*
- Wie B and Plescia C T 1984 Attitude stabilization of flexible spacecraft during stationkeeping maneuvers *J. Guid. Control Dyn.* **7** 430–6
- Zhao Y and Jones B 1997 Pulse width modulated reinforced piezo air jet actuators *Mechatronics* **7** 11–25